

Progress Towards Submersible Microrobots: A Novel 13-mg Low-Power SMA-Based Actuator for Underwater Propulsion

Cody R. Longwell, Conor K. Trygstad, Francisco M. F. R. Gonçalves, Ke Xu, and Néstor O. Pérez-Arancibia

Abstract—We introduce a new low-power 13-mg microactuator driven by *shape-memory alloy* (SMA) wires for underwater operation. The development of this device was motivated by the recent creation of microswimmers such as the FRISHBot, WaterStrider, VLEIBot, VLEIBot⁺, and VLEIBot⁺⁺. The first four of these robots, ranging from 30 to 90 mg, function tethered to an electrical power supply while the last platform is an 810-mg fully autonomous system. These five robots are driven by *dry* SMA-based microactuators first developed for microrobotic crawlers such as the SMALLBug and SMARTI. As shown in this abstract, dry SMA-based actuators do not operate efficiently under water due to high heat-transfer rates in this medium; for example, the actuators that drive the VLEIBot⁺⁺ require about 40 mW of average power at 1 Hz in dry air while requiring about 900 mW of average power at 1 Hz in water. In contrast, the microactuator presented in this abstract consumes about 150 mW of average power at 1 Hz in both dry air and water; additionally, it can be excited directly using an onboard battery through simple power electronics implemented on a custom-built *printed circuit board* (PCB). This technological breakthrough was enabled by the integration of a soft structure that encapsulates the SMA wires that drive the actuator in order to passively control the rates of heat transfer. The results presented here represent preliminary, yet compelling, experimental evidence that the proposed actuation approach will enable the development of fully autonomous and controllable submersible microswimmers. To accomplish this objective, we will evolve the current version of the VLEIBot⁺⁺ and introduce new bioinspired underwater propulsion mechanisms.

I. INTRODUCTION

Submersible aquatic microrobots have significant potential to assist humans with complex tasks, including search and rescue, ecological monitoring, surveillance, underwater inspection of infrastructure and machinery, maintenance of aquaculture instrumentation and facilities, and automated pest control in hydroponic agriculture. For this vision to become a reality, the microswimmers must operate autonomously, have structural and behavioral robustness, and be resilient against environmental uncertainty. The recent development of novel *high-work-density* (HWD) microactuators driven by *shape-memory alloy* (SMA) wires enabled the creation of numerous locomoting microrobots with new capabilities—for example, see [1]–[7]. The newest of these robotic systems is the VLEIBot⁺⁺ surface swimmer shown in Fig. 1, which weighs 810 mg, is driven by *dry* SMA-based actuators, and can function autonomously from both the power and control perspectives (see accompanying supplementary movie). Preliminary experiments indicate that due to high heat-transfer rates in water and associated power inefficiencies, the dry actuators that drive the VLEIBot⁺⁺ are not well suited to propel submersible swimmers. To accurately understand these phenomena, we designed and performed experiments that quantify the power requirements

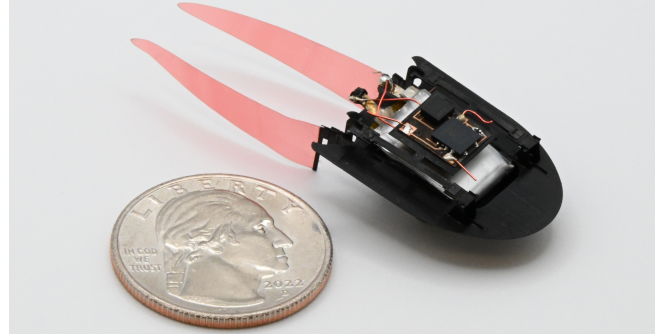


Fig. 1. **Photograph of the VLEIBot⁺⁺.** This microrobot is an 810-mg surface swimmer driven by a dry SMA-based actuator that can function autonomously from both the power and control perspectives (see accompanying supplementary movie).

for dry actuators to operate in air and water. Furthermore, we propose a new design for an actuator that can operate in air and water with approximately the same power requirements.

II. DRY ACTUATION AND POWER-CONSUMPTION CHARACTERIZATION IN AIR AND WATER

The dry microactuators that drive swimmers of the VLEIBot type, used in the research presented here and depicted at the top of Fig. 2(a), are made from carbon fiber, CuFR4 material, and SMA NiTi wires with a diameter of 38.1 μm and nominal transition temperature of 90 °C [5]. Given the thermal nature of SMA-based actuation, the corresponding energy and power requirements directly depend on heat-transfer phenomena. We quantified the power consumption of the tested actuators in air and water using the experimental setup shown in Fig. 2(b), which includes sensors that simultaneously measure electrical current (Adafruit, INA260) and actuator displacement (Keyence, LK 031). The actuators are excited using controlled *pulse-width modulation* (PWM) signals generated with the Mathworks Simulink real-time host–target system described in [4], [5]. This experimental setup was also used to quantify the power requirements of a new underwater HWD actuator with the basic design shown at the bottom of Fig. 2(a) and discussed in Section III. In preliminary experiments, we observed that using a laser displacement sensor through an acrylic pool and water, as shown in Fig. 2(c), distorts the obtained measurement. To understand and compensate for this effect, we estimated a dynamical model that maps the true signal into the distorted measurement by performing a discrete-time *linear time-invariant* (LTI) system identification procedure based on least-squares minimization and assuming an *infinite-impulse response* (IIR) structure (see Chapter 5.1.2 in [8]). Fig. 2(d) shows the frequency response of an identified IIR model with order 100. The input data used for system identification is frequency rich (persistently exciting) up to 5 Hz; therefore, we consider the Bode plot in Fig. 2(d) to be valid only at low frequencies (< 5 Hz). For all practical purposes, at low frequency, the identified system

This work was partially funded by the Washington State University (WSU) Foundation and the Palouse Club through a Cougar Cage Award to N. O. Pérez-Arancibia. Additional funding was provided by the WSU Voiland College of Engineering and Architecture through a start-up fund to N. O. Pérez-Arancibia.

C. R. Longwell and C. K. Trygstad contributed equally to this work.

The authors are with the School of Mechanical and Materials Engineering, Washington State University (WSU), Pullman, WA 99164, USA. Corresponding authors' e-mail: conor.trygstad@wsu.edu (C. K. T.); n.perezarancibia@wsu.edu (N. O. P.-A.).

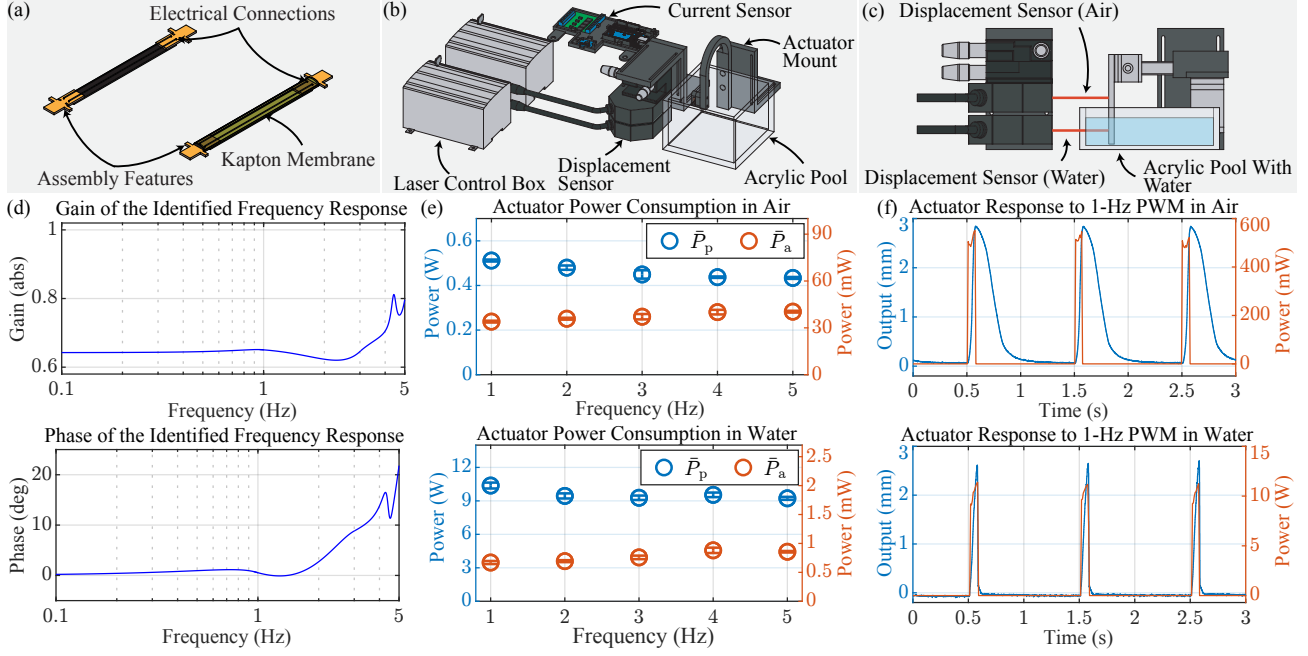


Fig. 2. **Experimental measurement of the power consumed by SMA-based microactuators during operation in air and water.** (a) Dry SMA-based microactuator developed to drive VLEIBot-like swimmers and characterized through the power experiments discussed in this abstract (top), and conceptual design of a low-power underwater SMA-based microactuator (bottom). (b) Experimental setup used to measure displacement and power consumption of the tested SMA-based microactuator in both air and water. The output displacement of the actuator is measured using a Keyence LK 031 laser sensor and the current used to compute power is measured using an Adafruit INA260 sensor. (c) Hardware configuration used to collect the data for identifying the system that maps the true actuation output to the measurement distorted by the path of the sensing laser (water and acrylic). (d) Identified model of the sensing system described in (c). (e) Mean and *experimental standard deviation* (ESD) of the average (\bar{P}_a) and peak (\bar{P}_p) power consumption of dry SMA-based actuator tested in air and water. (f) Actuator response and power consumption in air and water for a 1-Hz PWM excitation.

is simply a static mapping with a gain of 0.633. We further validated these findings using the linear regression function of the scikit-learn Python library to fit a *finite-impulse response* (FIR) filter with order 256.

In both air and water, we performed five types of power-consumption 32-second experiments corresponding to the PWM frequency-duty-cycle pairs, $\{f(i), DC(i)\}$, with the index $i \in \{1, \dots, 5\}$, for $f \in [1:1:5]$ Hz and $DC \in [7, 8, 9, 10, 10]\%$, while measuring and recording both the actuator output and electrical current, according to the scheme in Fig. 2(b). In air, we excited the actuator using a voltage—typically with a maximum value of 2.7 V—that nominally generates a maximum current of 250 mA through its SMA wires. In water, heuristically through simple experiments, we set a voltage that maximizes actuation output but is sufficiently low—typically with a maximum value of 12 V—such that the SMA wires of the device do not burn. After collecting the experimental data, we converted the currents into power signals according to $P(t) = I^2(t) \cdot R$, where respectively $I(t)$ and R are the measured instantaneous current flowing through the SMA wires of the device and total constant resistance of the actuator’s circuit (SMA + power wires), and t denotes time. For each experiment, we computed the average consumed power, \bar{P}_a , and peak power, \bar{P}_p , using 30 seconds of steady-state data. The estimated temperature of both media during all the experiments was on the order of 23 °C and the measured actuation outputs exceeded 2 mm at 1 Hz (see Fig. 2(f)).

For each tested PWM pair $\{f, DC\}$, we performed five back-to-back experiments; then, we computed the mean and *experimental standard deviation* (ESD) of both \bar{P}_a and \bar{P}_p . These data are summarized in Fig. 2(e), where \bar{P}_a and \bar{P}_p denote the means of P_a and P_p , respectively. Here, it can be seen that power consumption stays approximately constant with respect to actuation frequency. In air, \bar{P}_a and \bar{P}_p are on the order of 40 mW and 500 mW, for a

PWM excitation of 1 Hz; in water, \bar{P}_a and \bar{P}_p are on the order of 0.9 W and 10.7 W, for a PWM excitation of 1 Hz, which corresponds to a 2150 % increase in average power consumption with respect to the actuation-in-air case. This significant increase in power is explained by the additional energy required to Joule heat the SMA wires of the actuator under water due to the high heat-transfer coefficient of this medium. This phenomenon can be observed in the actuator responses shown in Fig. 2(f). In the actuation-in-air case, the instantaneous power, $P(t)$, remains below 600 mW while in the actuation-in-water case, the instantaneous power, $P(t)$, exceeds 10 W in three instances during the 3 seconds shown in the plot. Furthermore, the phase transition from *austenite* to *martensite* of the SMA material is drastically faster in water than in air due to the significantly higher cooling rate in the former medium than in the latter. Video footage showing the actuator functioning in both air and water can be seen in the accompanying supplementary movie.

III. NOVEL LOW-POWER SMA-BASED ACTUATION FOR UNDERWATER PROPULSION

To solve the problem of power for SMA-based microactuation in water, we propose the conceptual design depicted at the bottom of Fig. 2(a). The key element of this approach is an insulating air chamber made of Kapton that surrounds the SMA wires that drive the actuator, which locally reduces the heat-transfer coefficient of the system. Basic thermal analyses indicate that this design would drastically lower the power needed to efficiently generate SMA-based microactuation in water, thus enabling the development of submersible microswimmers. Using the same setup depicted in Fig. 2(b), we determined that a first-generation 13-mg prototype of this design can operate at a frequency of 1 Hz consuming only an average power of 150 mW with a peak of 1.6 W. This approach clearly shows a path towards autonomous underwater microrobotics.

REFERENCES

- [1] X. Yang, L. Chang, and N. O. Pérez-Arancibia, “An 88-milligram insect-scale autonomous crawling robot driven by a catalytic artificial muscle,” *Sci. Robot.*, vol. 5, no. 45, Aug. 2020, art. no. eaba0015.
- [2] X.-T. Nguyen, A. A. Calderón, A. Rigo, J. Z. Ge, and N. O. Pérez-Arancibia, “SMALLBug: A 30-mg Crawling Robot Driven by a High-Frequency Flexible SMA Microactuator,” *IEEE Robot. Automat. Lett.*, vol. 5, no. 4, pp. 6796–6803, Oct. 2020.
- [3] R. M. Bena, X.-T. Nguyen, A. A. Calderón, A. Rigo, and N. O. Pérez-Arancibia, “SMARTI: A 60-mg Steerable Robot Driven by High-Frequency Shape-Memory Alloy Actuation,” *IEEE Robot. Automat. Lett.*, vol. 6, no. 4, pp. 8173–8180, Oct. 2021.
- [4] C. K. Trygstad, X.-T. Nguyen, and N. O. Pérez-Arancibia, “A New 1-mg Fast Unimorph SMA-Based Actuator for Microrobotics,” in *Proc. IEEE/RSJ Int. Conf. Intell. Robots Syst. (IROS)*, Detroit, MI, USA, Oct. 2023, pp. 2693–2700.
- [5] E. K. Blankenship, C. K. Trygstad, F. M. F. R. Gonçalves, and N. O. Pérez-Arancibia, “VLEIBot: A New 45-mg Swimming Microrobot Driven by a Bioinspired Anguilliform Propulsor,” in *IEEE Int. Conf. Robot. Autom. (ICRA)*, Yokohama, Japan, May 2024, pp. 6014–6021.
- [6] C. K. Trygstad, E. K. Blankenship, and N. O. Pérez-Arancibia, “A New 10-mg SMA-Based Fast Bimorph Actuator for Microrobotics,” in *Proc. IEEE/RSJ Int. Conf. Intell. Robots Syst. (IROS)*, Abu Dhabi, UAE, Oct. 2024, to appear.
- [7] C. R. Longwell, C. K. Trygstad, and N. O. Pérez-Arancibia, “Testing the Waters: Actuation and Power for Insect-Scale Autonomous Underwater Vehicles,” submitted.
- [8] K. J. Keesman, *System Identification: An Introduction*. London, UK: Springer-Verlag, 2011.